

Dimension Reduction for Spatially Correlated Data: Spatial Predictor Envelope

Paul May^a and Hossein Moradi Rekabdarkolae^{b*}

^a *Department of Geographical Sciences, University of Maryland,*

^b *Department of Mathematics and Statistics,
South Dakota State University, Brookings, South Dakota.*

Abstract

Dimension reduction is an important tool for analyzing high-dimensional data. The predictor envelope is a method of dimension reduction for regression that assumes certain linear combinations of the predictors are immaterial to the regression. The method can result in substantial gains in estimation efficiency and prediction accuracy over traditional maximum likelihood and least squares estimates. While predictor envelopes have been developed and studied for independent data, no work has been done adapting predictor envelopes to spatial data. In this work, the predictor envelope is adapted to a popular spatial model to form the spatial predictor envelope (SPE). Maximum likelihood estimates for the SPE are derived, along with asymptotic distributions for the estimates given certain assumptions, showing the SPE estimates to be asymptotically more efficient than estimates of the original spatial model. The effectiveness of the proposed model is illustrated through simulation studies and the analysis of a geochemical data set.

Keyword: Dimension Reduction, Envelope model, Major chemical elements, Rare earth elements, Spatial correlation.

1 Introduction

Spatial linear regression is a popular approach to estimate and interpret the relationship between different spatial variables (Lambert et al., 2004; Beguería et al., 2013), or to assist the interpolation/prediction of a spatial response, as in the regression-kriging procedure (Hengl et al., 2007; Stein, 2012, Section 1.5). Estimates of the regression coefficients are often obtained via generalized least squares (GLS), which yields the maximum likelihood estimates for many spatial models (Mardia and Marshall, 1984). A large number of correlated predictors can result in high variance of the GLS estimates and subsequent poor prediction of the response. This is often addressed through dimension reduction, where the response is regressed on the predictors projected onto a lower-dimensional space. Many proposed methods of predictor dimension reduction for spatial regression are purely algorithmic. For example, Junttila and Laine (2017) used principal component regression, while Sampson et al. (2013) and Wijewardane et al. (2016) used partial least squares. These methods use algorithms for dimension reduction designed for independent data, only addressing the spatial correlation on the back-end, when regressing the response on the reduced predictors. Others have used a Bayesian approach: Taylor-Rodriguez et al. (2019) used a spatial factor model, where the response is linked to the predictors through a small number of latent spatial variables. In this paper, we propose a likelihood-based approach, called the spatial predictor envelope.

The predictor envelope (Cook et al., 2013) is a likelihood-based method of dimension reduction for regression that assumes certain linear combinations of the predictors are immaterial to the regression and therefore can be excluded. This can result in massive gains in efficiency for parameter estimation and prediction accuracy. In addition to predictor envelopes, many other envelope models have been developed. Lee and Su (2020) provide an extensive review of advances in envelope methods. Predictor envelopes have only been developed and studied assuming independent observations, an assumption often untenable for spatial data (Cressie, 2015). Rekabdarkolaei et al. (2020) proposed a spatial response envelope for regression with a multivariate spatial response that provides substantial advantages over the original response envelope for spatial data, as well as over other contemporary spatial models.

In this paper, we propose the spatial predictor envelope (SPE), providing a likelihood-based method for estimating the reduced predictor space and remaining model parameters. The model is an adaptation of the ‘separable’ multivariate spatial model (Mardia and Goodall, 1993), where the covariance between the response and predictors is of reduced rank via the predictor envelope. Maximum likelihood estimates (MLEs) are derived and the model and corresponding estimates are demonstrated through simulation and a data analysis. The simulations and data analysis are carried out with a univariate response, performing envelope dimension reduction on a multivariate predictor. However, the theory remains the same for a multivariate

response, with meaningful changes only in notation. Therefore, the theoretical developments of this paper allow for a multivariate response to keep the notation as general as possible.

Section 2 gives a brief review of predictor envelopes and spatial regression. Section 3 presents the SPE model and parameter MLEs. Section 4 discusses the potential gains over the original spatial regression model and asymptotic distributions of the parameter estimates. Section 5 provides simulation studies and Section 6 demonstrates a real data analysis on a geochemical data set. Some technical details and proofs are given in the Appendix.

2 Brief Review

In this section, the predictor envelope and spatial regression are briefly reviewed.

2.1 Predictor Envelopes

Consider the linear regression model

$$\vec{Y}|\vec{X} = \vec{\mu}_{Y|X} + \beta^T \vec{X} + \vec{\epsilon}_{Y|X}, \quad (1)$$

where \vec{Y} is an $r \times 1$ response, \vec{X} is a $p \times 1$ predictor, $\vec{\mu}_{Y|X}$ is an $r \times 1$ intercept vector, β is an $p \times r$ matrix of regression coefficients and $\vec{\epsilon}_{Y|X}$ is an $r \times 1$ error term with zero mean and constant variance. Under normality and iid

assumptions, the MLE for β is the ordinary least squares estimate. Predictor envelopes assume certain linear combinations of the predictors are invariant to changes in the response (Cook et al., 2013). Let \vec{Y} and \vec{X} be jointly multivariate normal. The envelope, $\mathcal{E} \subset \mathbb{R}^p$, is the smallest subspace of the predictor space such that

$$\mathbf{Q}_{\mathcal{E}}\vec{X}|\vec{Y} = \vec{y}_1 \sim \mathbf{Q}_{\mathcal{E}}\vec{X}|\vec{Y} = \vec{y}_2 \quad (2)$$

$$\mathbf{P}_{\mathcal{E}}\vec{X} \perp \mathbf{Q}_{\mathcal{E}}\vec{X}, \quad (3)$$

where $\mathbf{P}_{\mathcal{E}}$ and $\mathbf{Q}_{\mathcal{E}}$ are projections onto the envelope and orthogonal complement \mathcal{E}^{\perp} respectively. Orthogonality is with respect to the dot product, i.e. $\vec{A} \in \mathcal{E}, \vec{B} \in \mathcal{E}^{\perp}, \implies \vec{A}^T \vec{B} = 0$. The first condition declares the distribution of $\mathbf{Q}_{\mathcal{E}}\vec{X}$ to be invariant to changes in \vec{Y} . The second condition prevents $\mathbf{Q}_{\mathcal{E}}\vec{X}$ being affected by \vec{Y} through correlation with $\mathbf{P}_{\mathcal{E}}\vec{X}$. Assume the envelope \mathcal{E} is of dimension $u \leq p$. The previous conditions are equivalent to the parameterization:

$$\beta = \mathbf{\Gamma}_1 \eta \quad (4)$$

$$\text{Var}[\vec{X}] = \Sigma_X = \mathbf{\Gamma}_1 \mathbf{\Omega}_1 \mathbf{\Gamma}_1^T + \mathbf{\Gamma}_0 \mathbf{\Omega}_0 \mathbf{\Gamma}_0^T, \quad (5)$$

where $\mathbf{\Gamma}_1$ is a $p \times u$ orthogonal basis for \mathcal{E} , $\mathbf{\Gamma}_0$ is a $p \times (p - u)$ orthogonal basis for the orthogonal complement, η is a $u \times r$ matrix of coordinates for β with respect to $\mathbf{\Gamma}_1$, and $\mathbf{\Omega}_1$ and $\mathbf{\Omega}_0$ are covariance matrices representing

the variation within the envelope and orthogonal complement respectively. If $u = p$, no dimension reduction is performed and the model reverts to ordinary regression. If $u = 0$, then $\boldsymbol{\beta} = \mathbf{0}$ and no correlation exists between \vec{Y} and \vec{X} . Although particular bases $\boldsymbol{\Gamma}_1$ and $\boldsymbol{\Gamma}_0$ are not identifiable, the spaces they span are. Parameters $\boldsymbol{\Omega}_1$, $\boldsymbol{\Omega}_0$ and $\boldsymbol{\eta}$ are identifiable given a particular choice of basis for the envelope and its orthogonal complement. For fixed u , the model parameters are estimated from the data via maximum likelihood. The estimated dimension \hat{u} is selected via AIC, BIC or some other model selection technique.

Predictor envelopes improve estimation of $\boldsymbol{\beta}$ over ordinary least squares by reducing the parameter count and excluding small eigenvalues of $\boldsymbol{\Sigma}_X$ associated with dimensions within the orthogonal complement of \mathcal{E} that are therefore immaterial to the regression and needlessly inflating the variance of estimates. Predictor envelopes deliver the greatest gains when $\|\boldsymbol{\Omega}_0\| \ll \|\boldsymbol{\Omega}_1\|$, where $\|\cdot\|$ is the spectral norm. More information on predictor envelopes can be found in Cook et al. (2013), along with comparisons to other predictor reduction techniques.

Cook et al. (2013) derived MLEs for the predictor envelope parameters assuming independent observations. For spatial data, the assumption of independent observations is often untenable, as observations may be correlated based on their positions in space. Rekabdarkolaei et al. (2020) developed a spatial response envelope model, showing improvement over the traditional response envelope model of Cook et al. (2010) for spatially correlated data.

2.2 Spatial Regression

Let $\vec{Y}(s)$ be an $r \times 1$ response and $\vec{X}(s)$ a $p \times 1$ predictor, indexed by location $s \in D$, where D is a spatial domain, typically a subset of \mathbb{R}^2 . Assume the linear regression

$$\vec{Y}(s)|\vec{X}(s) = \vec{\mu}_{Y|X} + \boldsymbol{\beta}^T \vec{X}(s) + \vec{\epsilon}_{Y|X}(s), \quad s \in D. \quad (6)$$

Let the error term $\vec{\epsilon}_{Y|X}(s)$ be a Gaussian process with mean zero and separable covariance (Mardia and Goodall, 1993), i.e.

$$\text{Cov}[\vec{\epsilon}_{Y|X}(s), \vec{\epsilon}_{Y|X}(s')] = \rho_\theta(s, s') \boldsymbol{\Sigma}_{Y|X}, \quad s, s' \in D, \quad (7)$$

where $\boldsymbol{\Sigma}_{Y|X}$ is an $r \times r$ covariance matrix and $\rho_\theta(s, s')$ is a valid univariate correlation function (Genton, 2001), dependent on finite set of parameters θ . Given n observations of the response and predictors at locations $s_1, \dots, s_n \in D$, let

$$\mathbf{Y} = \begin{bmatrix} \vec{Y}(s_1)^T \\ \vdots \\ \vec{Y}(s_n)^T \end{bmatrix}, \quad \mathbf{X} = \begin{bmatrix} \vec{X}(s_1)^T \\ \vdots \\ \vec{X}(s_n)^T \end{bmatrix}, \quad \tilde{\mathbf{X}} = [\vec{\mathbf{1}}_n \quad \mathbf{X}] \quad (8)$$

be $n \times r$, $n \times p$ and $n \times (p + 1)$ matrices respectively, and $\boldsymbol{\rho}(\theta)$ be an $n \times n$ matrix where $[\boldsymbol{\rho}(\theta)]_{ij} = \rho_\theta(s_i, s_j)$. The MLEs for the intercept $\vec{\mu}_{Y|X}$ and

regression coefficients $\boldsymbol{\beta}$ are the generalized least squares (GLS) coefficients

$$[\hat{\mu}_{Y|X} \hat{\boldsymbol{\beta}}_{\text{GLS}}] = (\tilde{\mathbf{X}}^T \boldsymbol{\rho}(\hat{\theta})^{-1} \tilde{\mathbf{X}})^{-1} \tilde{\mathbf{X}}^T \boldsymbol{\rho}(\hat{\theta})^{-1} \mathbf{Y}, \quad (9)$$

where $\hat{\theta}$ is the maximum likelihood estimate for θ . The variance of $\hat{\boldsymbol{\beta}}_{\text{GLS}}$ is inversely proportionate to the magnitude of the eigenvalues of $(\tilde{\mathbf{X}}^T \boldsymbol{\rho}(\hat{\theta})^{-1} \tilde{\mathbf{X}})$ (see Theorem 1 in Section 4.1). Small eigenvalues can result in poor estimation and inaccurate prediction of the response. Projecting the predictors onto a subspace not associated with some of these small eigenvalues while preserving information relevant to the regression results in improved estimation of the regression parameters and prediction of the response.

Predictor envelopes estimate a reducing subspace for the predictors through the likelihood, requiring joint modeling of the predictors. Let the joint process of $\vec{Y}(s), \vec{X}(s)$ be a multivariate Gaussian process

$$\vec{Z}(s) = \begin{bmatrix} \vec{Y}(s) \\ \vec{X}(s) \end{bmatrix} = \vec{\mu}_Z + \vec{\epsilon}_Z(s), \quad s \in D, \quad (10)$$

where $\vec{\mu}_Z = [\vec{\mu}_X^T \vec{\mu}_Y^T]^T$ and $\vec{\epsilon}_Z(s)$ is a mean-zero Gaussian process with covariance

$$\text{Cov}[\vec{\epsilon}_Z(s), \vec{\epsilon}_Z(s')] = \rho_\theta(s, s') \boldsymbol{\Sigma}_Z, \quad \boldsymbol{\Sigma}_Z = \begin{bmatrix} \boldsymbol{\Sigma}_Y & \boldsymbol{\Sigma}_{XY}^T \\ \boldsymbol{\Sigma}_{XY} & \boldsymbol{\Sigma}_X \end{bmatrix}, \quad (11)$$

where $\boldsymbol{\Sigma}_{XY} = \boldsymbol{\Sigma}_X \boldsymbol{\beta}$. Note that this assumes $\vec{X}(s)$ has the same spatial

correlation function as $\vec{Y}(s)$. The MLE for β is still the GLS coefficients of Equation 9, however the MLE for θ will be effected by the joint modeling of $\vec{X}(s)$.

3 Spatial Predictor Envelope

In this section, we present the SPE model and parameter estimates.

3.1 Model

While the assumption of independent observations is convenient, it is problematic for data correlated over space (Cressie, 2015). The predictor envelope can be adapted to spatial data by assuming the data follows the joint spatial model in Equation 10, but with the envelope parameterization of Conditions 4 and 5:

$$\begin{aligned} \Sigma_X &= \Gamma_1 \Omega_1 \Gamma_1^T + \Gamma_0 \Omega_0 \Gamma_0^T \quad \text{and} \quad \Sigma_{XY} = \Gamma_1 \Omega_1 \eta \\ &\implies \beta = \Gamma_1 \eta, \end{aligned} \tag{12}$$

where the the envelope parameters are the same as those defined in Section 2. Throughout the paper, the model presented in Equation 10 that satisfies Conditions 12 is called the **spatial predictor envelope** (SPE). If $u = p$, no dimension reduction is performed and the model is equivalent to the unconstrained, full spatial regression of Equation 10. If $u = 0$, then $\Sigma_{XY} = \beta = \mathbf{0}$, implying $\vec{Y}(s)$ and $\vec{X}(s)$ are independent Gaussian processes. But

if $0 < u < p$, then Σ_{XY} and β are of reduced rank, with column vectors contained within the envelope space $\mathcal{E} = \text{span}(\Gamma_1)$. In this case, efficiency gains in estimation of β are possible through a reduced parameter count and omission of small eigenvalues of Σ_X (see Section 4.1). If spatial parameters θ and envelope dimension u are known, then the SPE is always asymptotically efficient versus the full spatial regression (see Section 4.2).

The conditional distribution $\vec{Y}(s)|\vec{X}(s)$ provides a more typical spatial regression format for the SPE

$$\begin{aligned}\vec{Y}(s)|\vec{X}(s) &= \vec{\mu}_{Y|X} + \beta^T \vec{X}(s) + \vec{\epsilon}_{Y|X}(s) \\ &= \vec{\mu}_{Y|X} + (\Gamma_1 \eta)^T \vec{X}(s) + \vec{\epsilon}_{Y|X}(s),\end{aligned}\tag{13}$$

where $\vec{\epsilon}_{Y|X}(s)$ is a mean-zero Gaussian process of dimension r with covariance

$$\begin{aligned}\text{Cov}[\vec{\epsilon}_{Y|X}(s), \vec{\epsilon}_{Y|X}(s')] &= \rho_\theta(s, s') \Sigma_{Y|X} \\ \Sigma_{Y|X} &= \Sigma_Y - \Sigma_{XY}^T \Sigma_X^{-1} \Sigma_{XY} \\ &= \Sigma_Y - \eta^T \Omega_1 \eta.\end{aligned}\tag{14}$$

While this conditional formulation is useful for interpretation and prediction, the joint formulation of Equation 10 is used for parameter estimation, as the envelope parameters affect the distribution of $\vec{X}(s)$.

3.2 Maximum Likelihood Estimation

Let \mathbf{Y} , \mathbf{X} , $\tilde{\mathbf{X}}$, and $\boldsymbol{\rho}(\theta)$ be the observation matrices defined in Equation 8, and let $\tilde{\mathbf{Y}} = [\tilde{\mathbf{I}} \mathbf{Y}]$. For fixed envelope dimension u , the maximum likelihood estimates for the SPE are

$$\begin{aligned} \hat{\boldsymbol{\Gamma}}_1, \hat{\theta} = \underset{\mathbf{G}_1, \phi}{\operatorname{argmin}} \{ & n \log |\mathbf{G}_1^T \mathbf{S}_{X|Y}(\phi) \mathbf{G}_1| + n \log |\mathbf{G}_1^T \mathbf{S}_X^{-1}(\phi) \mathbf{G}_1| \\ & + n \log |\mathbf{S}_X(\phi)| + n \log |\mathbf{S}_Y(\phi)| + (r + p) \log |\boldsymbol{\rho}(\phi)| \}, \end{aligned} \quad (15)$$

where \mathbf{G}_1 is a $p \times u$ orthogonal matrix representing $\boldsymbol{\Gamma}_1$ during the optimization, ϕ is a potential set of spatial correlation parameters representing θ during the optimization, and

$$\begin{aligned} \mathbf{S}_{X|Y}(\phi) &= \left(\mathbf{X} - \tilde{\mathbf{Y}}(\tilde{\mathbf{Y}}^T \boldsymbol{\rho}(\phi)^{-1} \tilde{\mathbf{Y}})^{-1} \tilde{\mathbf{Y}}^T \boldsymbol{\rho}(\phi)^{-1} \mathbf{X} \right)^T \boldsymbol{\rho}(\phi)^{-1} \left(\mathbf{X} - \tilde{\mathbf{Y}}(\tilde{\mathbf{Y}}^T \boldsymbol{\rho}(\phi)^{-1} \tilde{\mathbf{Y}})^{-1} \tilde{\mathbf{Y}}^T \boldsymbol{\rho}(\phi)^{-1} \mathbf{X} \right) \\ \mathbf{S}_X(\phi) &= \left(\mathbf{X} - \tilde{\mathbf{I}}(\tilde{\mathbf{I}}^T \boldsymbol{\rho}(\phi)^{-1} \tilde{\mathbf{I}})^{-1} \tilde{\mathbf{I}}^T \boldsymbol{\rho}(\phi)^{-1} \mathbf{X} \right)^T \boldsymbol{\rho}(\phi)^{-1} \left(\mathbf{X} - \tilde{\mathbf{I}}(\tilde{\mathbf{I}}^T \boldsymbol{\rho}(\phi)^{-1} \tilde{\mathbf{I}})^{-1} \tilde{\mathbf{I}}^T \boldsymbol{\rho}(\phi)^{-1} \mathbf{X} \right) \\ \mathbf{S}_Y(\phi) &= \left(\mathbf{Y} - \tilde{\mathbf{I}}(\tilde{\mathbf{I}}^T \boldsymbol{\rho}(\phi)^{-1} \tilde{\mathbf{I}})^{-1} \tilde{\mathbf{I}}^T \boldsymbol{\rho}(\phi)^{-1} \mathbf{Y} \right)^T \boldsymbol{\rho}(\phi)^{-1} \left(\mathbf{Y} - \tilde{\mathbf{I}}(\tilde{\mathbf{I}}^T \boldsymbol{\rho}(\phi)^{-1} \tilde{\mathbf{I}})^{-1} \tilde{\mathbf{I}}^T \boldsymbol{\rho}(\phi)^{-1} \mathbf{Y} \right), \end{aligned} \quad (16)$$

$\mathbf{S}_{X|Y}(\phi)$, $\mathbf{S}_X(\phi)$ and $\mathbf{S}_Y(\phi)$ being sample covariances adjusted for parameters ϕ . The remaining parameter estimates are then

$$\begin{aligned} [\hat{\mu}_{Y|X} \hat{\boldsymbol{\beta}}_{\text{GLS}^*}] &= (\tilde{\mathbf{X}}^T \boldsymbol{\rho}(\hat{\theta})^{-1} \tilde{\mathbf{X}})^{-1} \tilde{\mathbf{X}}^T \boldsymbol{\rho}(\hat{\theta})^{-1} \mathbf{Y}, \quad \hat{\boldsymbol{\eta}} = \hat{\boldsymbol{\Gamma}}_1^T \hat{\boldsymbol{\beta}}_{\text{GLS}^*}, \quad \hat{\boldsymbol{\beta}} = \hat{\boldsymbol{\Gamma}}_1 \hat{\boldsymbol{\eta}}, \\ \hat{\boldsymbol{\Omega}}_1 &= \hat{\boldsymbol{\Gamma}}_1^T \mathbf{S}_X(\hat{\theta}) \hat{\boldsymbol{\Gamma}}_1, \quad \hat{\boldsymbol{\Omega}}_0 = \hat{\boldsymbol{\Gamma}}_0^T \mathbf{S}_X(\hat{\theta}) \hat{\boldsymbol{\Gamma}}_0. \end{aligned} \quad (17)$$

An asterisk is included in $\hat{\beta}_{\text{GLS}^*}$ to distinguish it from the traditional MLE, $\hat{\beta}_{\text{GLS}}$, because the estimate for θ is affected by joint estimation of $\mathbf{\Gamma}_1$. Derivation of the MLEs can be found in Appendix 8.1. Estimated dimension \hat{u} can be chosen via AIC, BIC or cross-validation. It is suggested that BIC or cross-validation be used when prediction of the response is the goal, and AIC when a more conservative dimension reduction is desired.

Objective Function 15 requires optimization over $p \times u$ orthogonal \mathbf{G}_1 . The reparameterization of Cook et al. (2016) can be applied for an unconstrained optimization: Without loss of generality, let the rows of \mathbf{G}_1 be ordered such that the $u \times u$ matrix \mathbf{G}_{11} formed by the first u rows is non-singular. Such an ordering must exist, because $\text{rank}(\mathbf{G}_1) = u$. Then

$$\mathbf{G}_1 = \begin{bmatrix} \mathbf{G}_{11} \\ \mathbf{G}_{12} \end{bmatrix} = \begin{bmatrix} \mathbf{I}_u \\ \mathbf{A} \end{bmatrix} \mathbf{G}_{11} = \mathbf{C}_A \mathbf{G}_{11}, \quad (18)$$

where $\mathbf{A} = \mathbf{G}_{12} \mathbf{G}_{11}^{-1}$ is an unconstrained $(p - u) \times u$ matrix and $\mathbf{C}_A = [\mathbf{I}_u \ \mathbf{A}^T]^T$. Note that since the columns of \mathbf{G}_1 are linear combinations of the columns of \mathbf{C}_A , and vice-versa, the two matrices have the same column space. Making the substitution given by Equation 18 in Objective Function

15 yields

$$\begin{aligned} \hat{\mathbf{A}}, \hat{\theta} = \operatorname{argmin}_{\mathbf{A}, \phi} \{ & n \log |\mathbf{C}_{\mathbf{A}}^T \mathbf{S}_{X|Y}(\phi) \mathbf{C}_{\mathbf{A}}| + n \log |\mathbf{C}_{\mathbf{A}}^T \mathbf{S}_X^{-1}(\phi) \mathbf{C}_{\mathbf{A}}| - 2n \log |\mathbf{C}_{\mathbf{A}}^T \mathbf{C}_{\mathbf{A}}| \\ & + n \log |\mathbf{S}_X(\phi)| + n \log |\mathbf{S}_Y(\phi)| + (r + p) \log |\boldsymbol{\rho}(\phi)| \}. \end{aligned} \quad (19)$$

Then any off-the-shelf optimization routine can be applied over the unconstrained $\{\phi, \mathbf{A}\}$, applying any necessary transformation to ensure ϕ is unconstrained. Typically the spatial correlation parameters are strictly positive, so a log-transformation will suffice. To reclaim the orthogonal parameterization $\hat{\boldsymbol{\Gamma}}_1$ after the optimization is complete, take any orthogonal basis for the column space of $\mathbf{C}_{\hat{\mathbf{A}}}$, for example, the eigenvectors with non-zero eigenvalues of $\mathbf{C}_{\hat{\mathbf{A}}} \mathbf{C}_{\hat{\mathbf{A}}}^T$. The original, constrained Objective Function 15 can also be optimized using routines with orthogonality constraints, such as Wen and Yin (2013) which is implemented in ‘R’ package ‘rstiefel’ (Hoff and Franks, 2019; R Core Team, 2019).

4 Theoretical Results

In this section, we present the potential gains and asymptotic distributions of the SPE model parameters.

4.1 Potential Gains

General finite sample variances of $\hat{\boldsymbol{\beta}}$ are not readily available for the SPE model. However, if we assume some of the nuisance parameters are known, finite sample variances can be derived that are instructive to the potential gains of the SPE model over the full spatial regression.

Theorem 1. Assume the envelope and corresponding basis $\boldsymbol{\Gamma}_1$ are known, as well as spatial parameters θ . The variance of the SPE estimates $\hat{\boldsymbol{\beta}}$ are

$$\text{Var}[\text{vec}(\hat{\boldsymbol{\beta}})] = \left(\frac{1}{n - u - 2} \right) \boldsymbol{\Sigma}_{Y|X} \otimes \boldsymbol{\Gamma}_1 \boldsymbol{\Omega}_1^{-1} \boldsymbol{\Gamma}_1^T. \quad (20)$$

Proof of Theorem 1 can be found in Appendix 8.2. The following corollary provides the potential gains over the full spatial regression.

Corollary 1. Given the assumptions of Theorem 1, the variance of the full spatial regression (GLS) estimates $\hat{\boldsymbol{\beta}}_{\text{GLS}}$ are

$$\text{Var}[\text{vec}(\hat{\boldsymbol{\beta}}_{\text{GLS}})] = \left(\frac{1}{n - p - 2} \right) \boldsymbol{\Sigma}_{Y|X} \otimes \boldsymbol{\Sigma}_X^{-1}, \quad (21)$$

which implies the variance of the SPE estimates can be written as

$$\text{Var}[\text{vec}(\hat{\boldsymbol{\beta}})] = \left(\frac{n - p - 2}{n - u - 2} \right) \text{Var}[\text{vec}(\hat{\boldsymbol{\beta}}_{\text{GLS}})] - \left(\frac{1}{n - u - 2} \right) \boldsymbol{\Sigma}_{Y|X} \otimes \boldsymbol{\Gamma}_0 \boldsymbol{\Omega}_0^{-1} \boldsymbol{\Gamma}_0^T. \quad (22)$$

By the previous corollary, the potential gains of the SPE over GLS are proportionate to the parameter reduction and inversely proportionate to the

magnitude of $\mathbf{\Omega}_0$. While gains made through parameter reduction can be significant, especially for relatively small sample sizes, the greatest gains are possible via the omission of small eigenvalues in $\mathbf{\Omega}_0$.

4.2 Asymptotic Distributions

In this section, it is assumed that spatial parameters θ are known, and the asymptotic distributions of the SPE parameter estimates are studied and compared to that of the unconstrained, full spatial regression model of Equation 10 with no dimension reduction. Under the assumption of known θ , the asymptotic variances of the SPE are equivalent in form to those of the traditional predictor envelope.

Asymptotic variance of the estimates are not directly available through inversion of the Fisher Information matrix because $\mathbf{\Gamma}_1$ is over parameterized: there are multiple possibilities for the $p \cdot u$ entries in matrix $\mathbf{\Gamma}_1$ that lead to an orthogonal basis for the same space, and therefore give equivalent models. The techniques of Cook et al. (2010, 2013) are followed, applying the results of Shapiro (1986) for deriving asymptotic variances of over-parameterized models. Let

$$\psi = \begin{bmatrix} \text{vech}(\mathbf{\Sigma}_{Y|X}) \\ \text{vec}(\mathbf{\Gamma}_1) \\ \text{vech}(\mathbf{\Omega}_1) \\ \text{vech}(\mathbf{\Omega}_0) \end{bmatrix}$$

and $h(\psi)$ be a vector of the estimable parameters

$$h(\psi) = \begin{bmatrix} \text{vech}(\boldsymbol{\Sigma}_{Y|X}) \\ \text{vech}(\boldsymbol{\Sigma}_X) \\ \text{vec}(\boldsymbol{\beta}) \end{bmatrix}.$$

Intercept $\vec{\mu}_Z$ is omitted because its estimates are asymptotically independent of the others. Let \mathbf{H} be the gradient matrix $[\mathbf{H}]_{ij} = \frac{\partial h_i}{\partial \psi_j}$ and let \mathbf{J}_F be the Fisher Information matrix of $h(\psi)$ under the unconstrained model of Equation 10. Under the assumption of known θ , the parameter estimates for the unconstrained model are consistent and asymptotically normal with variance \mathbf{J}_F^{-1} (more details in Appendix 8.3). Then by (Shapiro, 1986, Proposition 4.1) the following theorem results

Theorem 2. Assume spatial parameters θ are known. Then $h(\hat{\psi}) \rightarrow N(h(\psi), \mathbf{J}_{\text{SPE}}^{-1})$, where

$$\text{avar}[\sqrt{n}h(\psi)] \equiv \mathbf{J}_{\text{SPE}}^{-1} = \mathbf{H}(\mathbf{H}^T \mathbf{J}_F \mathbf{H})^\dagger \mathbf{H}^T, \quad (23)$$

where \dagger is the Moore-Penrose inverse. In particular, the asymptotic variances for parameter estimates $\boldsymbol{\beta}$ are

$$\text{avar}[\sqrt{n}\text{vec}(\hat{\boldsymbol{\beta}})] = \boldsymbol{\Sigma}_{Y|X} \otimes \boldsymbol{\Gamma}_1 \boldsymbol{\Omega}_1^{-1} \boldsymbol{\Gamma}_1^T + (\boldsymbol{\eta}^T \otimes \boldsymbol{\Gamma}_0) \mathbf{M}^{-1} (\boldsymbol{\eta} \otimes \boldsymbol{\Gamma}_0^T), \quad (24)$$

where

$$\mathbf{M} = \boldsymbol{\eta} \boldsymbol{\Sigma}_{Y|X}^{-1} \boldsymbol{\eta}^T \otimes \boldsymbol{\Omega}_0 + \boldsymbol{\Omega}_1 \otimes \boldsymbol{\Omega}_0^{-1} + \boldsymbol{\Omega}_1^{-1} \otimes \boldsymbol{\Omega}_0 - 2\mathbf{I}_u \otimes \mathbf{I}_{p-u}.$$

These asymptotic variances are the same as those of the traditional predictor envelope (Cook et al., 2013). Note that when these formulae are used in practice, the plug-in estimates of the asymptotic variance will use the MLEs for the SPE model, which can differ greatly than those of the traditional predictor envelope model.

The next theorem declares the SPE estimates are asymptotically efficient compared to the full spatial regression (GLS) estimates.

Theorem 3. Let J_F^{-1} be the asymptotic variance for the full regression model and J_{SPE}^{-1} be the asymptotic variance for the SPE estimates given by Equation 23. Then

$$\mathbf{J}_F^{-1} - \mathbf{J}_{\text{SPE}}^{-1} \geq 0.$$

Proof of Theorem 3 is in the Appendix. In Section 5, the asymptotic distributions for $\hat{\boldsymbol{\beta}}$ given by Equation 24 are compared to the empirical distribution of simulation estimates of $\boldsymbol{\beta}$, where θ is estimated from the data for every sample. The two distributions match each other well, suggesting the above asymptotic variances are useful in practice.

5 Simulations

Simulations 1 and 2 present scenarios advantageous to the SPE, where Simulation 1 assumes envelope dimension u is known and fixed to study estimation of $\mathbf{\Gamma}_1$ and Simulation 2 assumes u is unknown to study dimension selection and estimation of $\boldsymbol{\beta}$. Simulations 3 and 4 present scenarios where the SPE provides no advantage over traditional spatial regression (GLS). Simulation 5 compares the asymptotic distributions of Equation 24 to the empirical distribution of the SPE regression estimates $\hat{\boldsymbol{\beta}}$.

Simulation 1: The accuracy of envelope subspace estimation from objective function 15 is compared to the envelope subspace estimation in Cook et al. (2013, 2016). The response $\vec{Y}(s)$ and predictors $\vec{X}(s)$ are simulated at n locations s_1, \dots, s_n according to the SPE model, given by Equation 10 subject to the envelope conditions 12. For this first simulation, envelope dimension u is assumed to be known. The data dimensions are $p = 10$, $u = 3$, $r = 1$, and the model parameters are $\mathbf{\Omega}_1 = \text{diag}\{\exp(-1^{2/3}), \exp(-2^{2/3}), \exp(-3^{2/3})\}$, $\mathbf{\Omega}_0 = \text{diag}\{\exp(-4^{2/3}), \exp(-5^{2/3}), \dots, \exp(-10^{2/3})\}$, $\boldsymbol{\eta} = [1 \ 1 \ 1]^T$, $\boldsymbol{\Sigma}_{Y|X} = 0.05$. These particular data dimensions are chosen to mirror the data analysis in Section 6 and parameters $\mathbf{\Omega}_1, \mathbf{\Omega}_0$ are chosen such that $\|\mathbf{\Omega}_0\| \ll \|\mathbf{\Omega}_1\|$, presenting a scenario advantageous to predictor envelopes. Basis $\mathbf{\Gamma}_1$ is randomly generated every iteration according to the methods of Mezzadri (2006) using the ‘R’ package ‘pracma’ (Borchers, 2019; R Core Team, 2019), and spatial coordinates are randomly generated according to a uniform distribution on

$[0, 1] \times [0, 1]$ every iteration. An exponential correlation function with white noise is used

$$\rho(s, s') = \tau 1_{s=s'} + (1 - \tau) \exp\left(-\frac{\|s - s'\|}{\lambda}\right), \quad (25)$$

where $\tau \in [0, 1]$ controls the proportion of noise relative to the spatial variation and $\lambda \in \mathbb{R}^+$ is a range parameter. We used $\tau = 0.1$ and $\lambda = 0.3$, giving the data substantial spatial correlation. The simulation is repeated 500 times for $n = 50, 100, 200$ respectively. Models are compared by the angle between the estimated and true envelope space, $\angle\{\text{span}(\hat{\Gamma}_1), \text{span}(\Gamma_1)\}$, and the squared Euclidean distance between the estimated and true regression coefficients $\|\hat{\beta} - \beta\|^2$. The angle between two subspaces of equal dimension with orthogonal bases \mathbf{A} and \mathbf{B} respectively is computed as the arc-cosine of the largest singular value of $\mathbf{A}^T \mathbf{B}$, which is equivalent to the largest principal angle between the subspaces (Björck and Golub, 1973). Simulation results are provided in Table 1. The SPE improves estimation of $\text{span}(\Gamma_1)$ and β over the traditional predictor envelope by accounting for the spatial correlation. The SPE improves estimation of $\hat{\beta}$ over the full spatial regression by excluding the small eigenvalues in Ω_0 .

Simulation 2: Data is simulated according to the same parameters as Simulation 1, but u is estimated via BIC. Table 2 gives average errors $\|\hat{\beta} - \beta\|^2$ and Figure 4 in Appendix 8.4 gives histograms of selected envelope dimension \hat{u} . The SPE improves estimation of $\hat{\beta}$ over the traditional predictor

Table 1: Average error between estimated and true subspace, $\angle\{\text{span}(\hat{\mathbf{\Gamma}}_1), \text{span}(\mathbf{\Gamma}_1)\}$, and average squared error of regression coefficients, $\|\hat{\boldsymbol{\beta}} - \boldsymbol{\beta}\|^2$. Standard deviations of the average are in parentheses.

| n | Error Metric | SPE | PE | GLS |
|-----|--|-----------------|---------------|---------------|
| 50 | $\angle\{\text{span}(\hat{\mathbf{\Gamma}}_1), \text{span}(\mathbf{\Gamma}_1)\}$ | 0.082 (0.001) | 0.130 (0.003) | NA |
| | $\ \hat{\boldsymbol{\beta}} - \boldsymbol{\beta}\ ^2$ | 0.144 (0.009) | 0.361 (0.018) | 0.530 (0.017) |
| 100 | $\angle\{\text{span}(\hat{\mathbf{\Gamma}}_1), \text{span}(\mathbf{\Gamma}_1)\}$ | 0.054 (< 0.001) | 0.114 (0.002) | NA |
| | $\ \hat{\boldsymbol{\beta}} - \boldsymbol{\beta}\ ^2$ | 0.047 (0.002) | 0.237 (0.012) | 0.206 (0.006) |
| 200 | $\angle\{\text{span}(\hat{\mathbf{\Gamma}}_1), \text{span}(\mathbf{\Gamma}_1)\}$ | 0.038 (< 0.001) | 0.108 (0.002) | NA |
| | $\ \hat{\boldsymbol{\beta}} - \boldsymbol{\beta}\ ^2$ | 0.022 (< 0.001) | 0.175 (0.007) | 0.093 (0.003) |

envelope and the full spatial regression, and improves selection of \hat{u} over the traditional predictor envelope. It appears that as $n \rightarrow \infty$, the SPE selects to true dimension via BIC with probability approaching one.

Table 2: Average error $\|\hat{\boldsymbol{\beta}} - \boldsymbol{\beta}\|^2$ with standard deviations in parentheses. Simulation scenario where $u < p$ and $\|\boldsymbol{\Omega}_0\| \ll \|\boldsymbol{\Omega}_1\|$.

| n | SPE | PE | GLS |
|-----|---------------|---------------|---------------|
| 50 | 0.221 (0.015) | 0.625 (0.030) | 0.530 (0.017) |
| 100 | 0.075 (0.004) | 0.443 (0.020) | 0.206 (0.006) |
| 200 | 0.029 (0.002) | 0.370 (0.014) | 0.093 (0.002) |

Simulation 3: Data is simulated according to the same parameters as Simulations 1 and 2, but $u = p = 10$, $\boldsymbol{\Omega}_1 = \text{diag}\{\exp(-1^{2/3}), \exp(-2^{2/3}), \dots, \exp(-10^{2/3})\}$ and $\boldsymbol{\eta} = [1 \dots 1]^T$, meaning $\boldsymbol{\Sigma}_X$ has small eigenvalues, but there is no proper envelope subspace. Envelope dimension is unknown and estimated via minimum BIC, giving the SPE an opportunity to falsely estimate a reducing subspace. Table 3 gives average errors $\|\hat{\boldsymbol{\beta}} - \boldsymbol{\beta}\|^2$ and Figure 5 in Appendix

8.4 gives histograms of selected envelope dimension \hat{u} . The SPE and GLS estimates perform similarly. The SPE often falsely estimates a reducing subspace via minimum BIC, but apparently not to the detriment (on average) of the regression estimates $\hat{\beta}$.

Table 3: Average error $\|\hat{\beta} - \beta\|^2$ with standard deviations in parentheses. Simulation scenario where $u = p$.

| n | SPE | PE | GLS |
|-----|---------------|---------------|---------------|
| 50 | 0.517 (0.018) | 0.970 (0.031) | 0.530 (0.017) |
| 100 | 0.213 (0.007) | 0.629 (0.021) | 0.206 (0.006) |
| 200 | 0.091 (0.003) | 0.475 (0.015) | 0.093 (0.002) |

Simulation 4: Data is simulated according to the same parameters as Simulations 1 and 2, but $\mathbf{\Omega}_1 = \text{diag}\{\omega_1, \omega_2, \omega_3\}$ and $\mathbf{\Omega}_0 = \text{diag}\{\omega_4, \dots, \omega_{10}\}$, where ω_j , $j = 1, \dots, 10$ are randomly generated according to a uniform distribution of $[0, 1]$ every iteration. In this way, the magnitudes of $\|\mathbf{\Omega}_1\|$ and $\|\mathbf{\Omega}_0\|$ are on average comparable. Table 4 gives average errors $\|\hat{\beta} - \beta\|^2$ and Figure 6 in Appendix 8.4 gives histograms of selected envelope dimension \hat{u} . The SPE provides no significant advantage over the GLS estimates in this scenario, due to the comparable magnitudes of $\|\mathbf{\Omega}_1\|$ and $\|\mathbf{\Omega}_0\|$.

Table 4: Average error $\|\hat{\beta} - \beta\|^2$ with standard deviations in parentheses. Simulation scenario where $u < p$ and $\|\mathbf{\Omega}_1\| \approx \|\mathbf{\Omega}_0\|$.

| n | SPE | PE | GLS |
|-----|---------------|---------------|---------------|
| 50 | 0.105 (0.015) | 0.189 (0.025) | 0.122 (0.016) |
| 100 | 0.040 (0.004) | 0.115 (0.013) | 0.042 (0.003) |
| 200 | 0.019 (0.003) | 0.151 (0.037) | 0.020 (0.002) |

Simulation 5: The asymptotic distributions for $\hat{\beta}$ given by Equation 24 are compared to the empirical distribution of simulation estimates of β where θ is estimated from the data for every sample. The model parameters are the same as Simulations 1 and 2, except that the basis $\mathbf{\Gamma}_1$ and the spatial coordinates are randomly generated once and held fixed throughout all 500 simulation iterations. In this way, the variance of $\hat{\beta}$ for a fixed model can be studied. For the same reason, u is considered known and fixed. The simulation is repeated for $n = 50, 100, 200$. Figure 1 gives histograms for the first estimated regression coefficient $\hat{\beta}_1$ with the asymptotic normal density given by Equation 24 plotted over-top. The empirical distributions and asymptotic distributions agree well, suggesting that the asymptotic distributions are useful in practice.

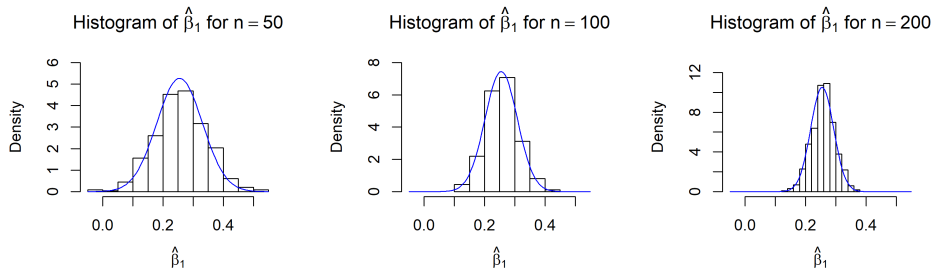


Figure 1: Histograms for the first estimated regression coefficient $\hat{\beta}_1$ across 500 simulation iterations with the asymptotic normal density given by Equation 24 plotted over-top.

6 Data Analysis

We analyze a geochemical data set to illustrate the spatial predictor envelope. The data set contains 53 samples of the concentrations of 11 major chemical elements and 17 rare earth elements (REEs) at 14 different locations across an oil and gas reserve in Wyoming (Quillinan et al., 2016). The data was collected to assess how rock type / major chemical element concentrations affected the concentration of REEs. REEs are critical to many modern technologies and industrial applications, but economically viable concentrations of REEs are uncommon and tend to occur in uncommon rock types (Van Gosen et al., 2019). There is interest in identifying general mineral characteristics that are correlated with high REE concentrations and using these correlations to identify REE mining prospects; see for example Lands (2014). We follow the techniques of Aitchison (1982) for compositional data, analyzing the log-ratios of the components. The log-concentrations of the 17 REEs are highly positively correlated, with over 95% of the variation explained by the first principal component. With few exceptions, REEs do not occur individually but vary in unison (Hoshino et al., 2016). Therefore, we used the total log-concentration of REEs as the univariate regression response, as it simplifies the model and remains in line with the data analysis goals. We used the log-concentrations of the major chemical elements as a multivariate regression predictor and the SPE to estimate a reducing subspace and linear relationship between the total REE log-concentration and major chemical

element log-concentrations. Appendix 8.5 contains more details and justifications on the choice of variables and data transformations. Figure 2 gives the locations and levels of sampled total REE log-concentrations.

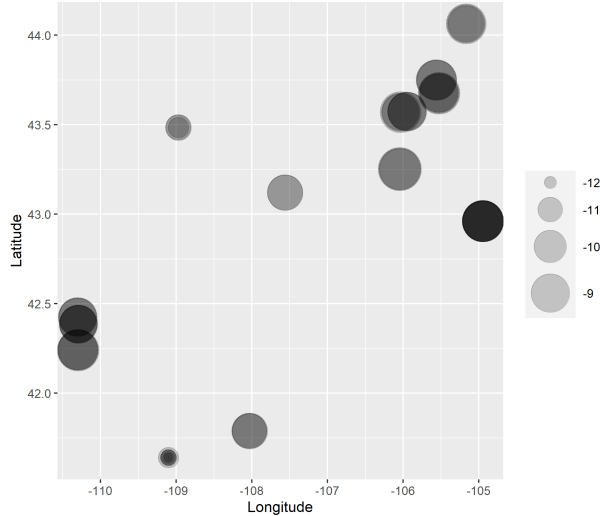


Figure 2: Locations and levels of sampled total REE log-concentrations.

An exponential correlation function with white noise (Equation 25) was used for all correlation functions. The SPE was fit to the data for $u = 0, \dots, p$ and the BIC scores were compared. Figure 3 gives a plot of BIC scores against dimension u . The SPE achieves a minimum BIC of 792 at $u = 3$. The BIC for the full spatial regression model is 817. For reference, the traditional predictor envelope of Cook et al. (2013), designed for independent observations, achieves a minimum BIC of 1197, also at $u = 3$. The substantially higher BIC score of the traditional predictor envelope when compared to the spatial models suggests accounting for the spatial correlation in this data is crucial. Table 5 gives the estimated coefficients, asymptotic standard errors and Z-

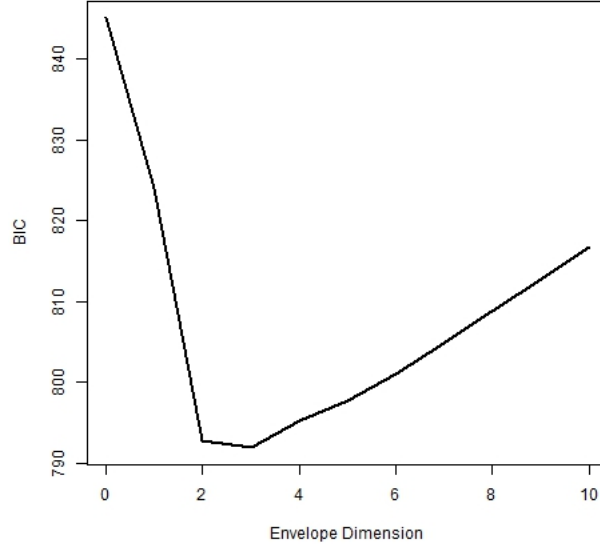


Figure 3: BIC scores for the SPE for $u = 0, \dots, p$. The SPE achieves a minimum of 792 at $u = 3$.

scores $\hat{\beta}_i / \sqrt{\text{avar}[\hat{\beta}_i]}$ for the SPE model with $u = 3$. Significant relationships are indicated between several major chemical concentrations and the total REE log-concentration, for example, a positive relationship for potassium oxide (K₂O) and phosphorus pentoxide (P₂O₅) and a negative relationship for magnesium oxide (MgO) and silicon dioxide (SiO₂). Alkaline igneous rocks are enriched in potassium and known to be hosts of REE deposits, providing an explanation for the strong positive relationship between potassium oxide and total REE log-concentration (Dostal, 2017).

To compare the predictive performance of the SPE against traditional spatial regression (GLS), a cross-validation study was performed on the data.

Table 5: Estimated coefficients, asymptotic standard errors and Z-scores $\hat{\beta}_i/\sqrt{\text{avar}[\hat{\beta}_i]}$ for each of the major chemical components.

| Chemical | CaO | Fe2O3 | K2O | LOI | MgO | MnO | Na2O | P2O5 | SiO2 | TiO2 |
|-------------------------------------|-------|-------|------|-------|-------|------|------|------|-------|------|
| $\hat{\beta}_i$ | -0.10 | -0.12 | 0.36 | -0.05 | -0.21 | 0.03 | 0.02 | 0.22 | -0.29 | 0.10 |
| $\sqrt{\text{avar}[\hat{\beta}_i]}$ | 0.08 | 0.09 | 0.08 | 0.09 | 0.07 | 0.07 | 0.06 | 0.09 | 0.10 | 0.10 |
| Z-score | -1.28 | -1.35 | 4.50 | -0.58 | -3.13 | 0.38 | 0.45 | 2.57 | -2.73 | 1.03 |

A hundred iterations of 10-fold cross-validation was performed, with predictions of the test data performed using the conditional expectation

$$\hat{Y}_{\text{test}} = E[Y_{\text{test}}|Y_{\text{train}}, \hat{\beta}, \hat{\theta}] = X_{\text{test}}\hat{\beta} + E[\epsilon_{\text{test}}|\epsilon_{\text{train}}, \hat{\theta}]$$

where the conditional expectation of the error terms is given by the kriging equation (Matheron, 1982; Cressie, 2015). The predictions were compared by their mean squared prediction error (MSPE), calculated as

$$\text{MSPE} = \frac{1}{N} \sum_{i=1}^N (\hat{Y}_{\text{test},i} - Y_{\text{test},i})^2,$$

where N is the number of predicted observations. The average MSPE for the SPE and spatial regression was 0.09 and 0.16 respectively, showing significant improvement in prediction through the dimension reduction of the predictors. For context, the sample variance of the response, $\frac{1}{n} \sum_{i=1}^n (Y_i - \bar{Y})^2$, is 1.31, meaning both methods predicted a substantial portion of the variation in the response.

7 Discussion

The proposed spatial predictor envelope provides an effective tool for multivariate spatial data. By reducing the dimension of the predictors through a likelihood-based approach, the SPE can improve estimation of the regression coefficients and prediction of the response over traditional spatial regression. The SPE improves estimation/prediction over the original predictor envelope for spatial data by accounting for spatial correlation.

In this paper, the asymptotic distribution for the estimable parameters is given for known spatial correlation parameters θ . The difficulty in deriving asymptotic distributions for unknown θ are two-fold. First, to apply the results of Shapiro (1986), a discrepancy function satisfying certain regularity conditions must be devised such that the parameters that minimize the discrepancy function are equivalent to the parameters that maximize the likelihood. Second, the results of Shapiro (1986) hinge upon the parameter estimates of the full, unconstrained model being consistent and asymptotically normal. This is a difficult problem in spatial statistics, where the answer often depends on the sampling scheme of the locations s_1, \dots, s_n and the spatial correlation function (Mardia and Marshall, 1984; Zhang, 2004).

The assumption of normality may be too restrictive for some applications. Cook and Zhang (2015) discuss envelope models in a generalized linear model context. Generalized linear mixed models are popular for modeling non-Gaussian spatial data, see for example Zhang (2002). Expanding spatial

envelopes to the general linear mixed model setting would be a worthy task.

References

John Aitchison. The statistical analysis of compositional data. *Journal of the Royal Statistical Society: Series B (Methodological)*, 44(2):139–160, 1982.

Santiago Beguería, Valentina Spanu, Ana Navas, Javier Machín, and Marta Angulo-Martínez. Modeling the spatial distribution of soil properties by generalized least squares regression: Toward a general theory of spatial variates. *Journal of soil and water conservation*, 68(3):172–184, 2013.

Ake Björck and Gene H Golub. Numerical methods for computing angles between linear subspaces. *Mathematics of computation*, 27(123):579–594, 1973.

Hans W. Borchers. *pracma: Practical Numerical Math Functions*, 2019. URL <https://CRAN.R-project.org/package=pracma>. R package version 2.2.5.

R Dennis Cook. *An introduction to envelopes: dimension reduction for efficient estimation in multivariate statistics*, volume 401. John Wiley & Sons, 2018.

R Dennis Cook and Xin Zhang. Foundations for envelope models and meth-

- ods. *Journal of the American Statistical Association*, 110(510):599–611, 2015.
- R Dennis Cook, Bing Li, and Francesca Chiaromonte. Envelope models for parsimonious and efficient multivariate linear regression. *Statistica Sinica*, pages 927–960, 2010.
- R Dennis Cook, Liliana Forzani, and Zhihua Su. A note on fast envelope estimation. *Journal of Multivariate Analysis*, 150:42–54, 2016.
- RD Cook, IS Helland, and Z Su. Envelopes and partial least squares regression. *Journal of the Royal Statistical Society: Series B (Statistical Methodology)*, 75(5):851–877, 2013.
- Noel Cressie. *Statistics for spatial data*. John Wiley & Sons, 2015.
- Jaroslav Dostal. Rare Earth Element Deposits of Alkaline Igneous Rocks. *Resources*, 6:34, 07 2017. doi: 10.3390/resources6030034.
- Marc G Genton. Classes of kernels for machine learning: a statistics perspective. *Journal of machine learning research*, 2(Dec):299–312, 2001.
- Tomislav Hengl, Gerard BM Heuvelink, and David G Rossiter. About regression-kriging: From equations to case studies. *Computers & geosciences*, 33(10):1301–1315, 2007.
- Peter Hoff and Alexander Franks. *rstiefel: Random Orthonormal Matrix*

- Generation and Optimization on the Stiefel Manifold*, 2019. URL <https://CRAN.R-project.org/package=rstiefel>. R package version 1.0.0.
- M. Hoshino, K. Sanematsu, and Y. Watanabe. Chapter 279 - REE Mineralogy and Resources. In Bünzli Jean-Claude and Pecharsky Vitalij K., editors, *Including Actinides*, volume 49 of *Handbook on the Physics and Chemistry of Rare Earths*, pages 129–291. Elsevier, 2016. doi: <https://doi.org/10.1016/bs.hpre.2016.03.006>. URL <https://www.sciencedirect.com/science/article/pii/S0168127316300010>.
- Virpi Junttila and Marko Laine. Bayesian principal component regression model with spatial effects for forest inventory variables under small field sample size. *Remote Sensing of Environment*, 192:45–57, 2017.
- Dayton M Lambert, James Lowenberg-Deboer, and Rodolfo Bongiovanni. A comparison of four spatial regression models for yield monitor data: A case study from argentina. *Precision Agriculture*, 5(6):579–600, 2004.
- Utah Trust Lands. Rare earth element prospects and occurrences in Utah. Technical report, Utah Geological Survey, 01 2014.
- Minji Lee and Zhihua Su. A review of envelope models. *International Statistical Review*, 88(3):658–676, 2020.
- Kanti V Mardia and Colin R Goodall. Spatial-temporal analysis of multivariate environmental monitoring data. *Multivariate environmental statistics*, 6(76):347–385, 1993.

- Kanti V Mardia and Roger J Marshall. Maximum likelihood estimation of models for residual covariance in spatial regression. *Biometrika*, 71(1): 135–146, 1984.
- G. Matheron. Pour une Analyse Krigeante des Données Régionalisées. *Cent. de Geostat*, 1982.
- Francesco Mezzadri. How to generate random matrices from the classical compact groups. *arXiv preprint math-ph/0609050*, 2006.
- Scott Quillinan, Charles Nye, Travis McLing, and Hari Neupane. Rare Earth Element Geochemistry for Produced Waters, WY. 6 2016. doi: 10.15121/1360765. URL <https://www.osti.gov/biblio/1360765>.
- R Core Team. *R: A Language and Environment for Statistical Computing*. R Foundation for Statistical Computing, Vienna, Austria, 2019. URL <https://www.R-project.org/>.
- Hossein Moradi Rekabdarkolae, Qin Wang, Zahra Naji, and Montserrat Fuentes. New parsimonious multivariate spatial model: Spatial envelope. *Statistica Sinica*, 30(3), 2020.
- Paul D Sampson, Mark Richards, Adam A Szpiro, Silas Bergen, Lianne Sheppard, Timothy V Larson, and Joel D Kaufman. A regionalized national universal kriging model using Partial Least Squares regression for estimating annual PM_{2.5} concentrations in epidemiology. *Atmospheric environment*, 75:383–392, 2013.

- Alexander Shapiro. Asymptotic theory of overparameterized structural models. *Journal of the American Statistical Association*, 81(393):142–149, 1986.
- Michael L Stein. *Interpolation of spatial data: some theory for kriging*. Springer Science & Business Media, 2012.
- Daniel Taylor-Rodriguez, Andrew O Finley, Abhirup Datta, Chad Babcock, Hans-Erik Andersen, Bruce D Cook, Douglas C Morton, and Sudipto Banerjee. Spatial factor models for high-dimensional and large spatial data: An application in forest variable mapping. *Statistica Sinica*, 29: 1155, 2019.
- Bradley S Van Gosen, Philip L Verplanck, and Poul Emsbo. Rare earth element mineral deposits in the United States. Technical report, US Geological Survey, 2019.
- Zaiwen Wen and Wotao Yin. A feasible method for optimization with orthogonality constraints. *Mathematical Programming*, 142(1-2):397–434, 2013.
- Nuwan K Wijewardane, Yufeng Ge, Skye Wills, and Terry Loecke. Prediction of soil carbon in the conterminous United States: Visible and near infrared reflectance spectroscopy analysis of the rapid carbon assessment project. *Soil Science Society of America Journal*, 80(4):973–982, 2016.
- Hao Zhang. On estimation and prediction for spatial generalized linear mixed models. *Biometrics*, 58(1):129–136, 2002.

Hao Zhang. Inconsistent estimation and asymptotically equal interpolations in model-based geostatistics. *Journal of the American Statistical Association*, 99(465):250–261, 2004.

8 Appendix

8.1 Maximum Likelihood Estimation

Let \mathbf{Y} and \mathbf{X} be $n \times r$ and $n \times p$ matrices of observations at locations s_1, \dots, s_n and $\boldsymbol{\rho}(\theta)$ be the $n \times n$ correlation matrix where $\boldsymbol{\rho}(\theta)_{ij} = \rho_\theta(s_i, s_j)$. Let $\vec{1}$ be a $n \times 1$ vector of ones and $\tilde{\mathbf{Y}} = [\vec{1} \ \mathbf{Y}]$, $\tilde{\mathbf{X}} = [\vec{1} \ \mathbf{X}]$. Assume the envelope dimension u is known.

Derivation of the estimates is easiest if the joint log-likelihood $L(\mathbf{X}, \mathbf{Y})$ is decomposed into $L(\mathbf{X}, \mathbf{Y}) = L(\mathbf{X}|\mathbf{Y}) + L(\mathbf{Y})$. First, see that

$$\begin{aligned} \boldsymbol{\Sigma}_{X|Y} &= \boldsymbol{\Sigma}_X - \boldsymbol{\Sigma}_{XY} \boldsymbol{\Sigma}_Y^{-1} \boldsymbol{\Sigma}_{XY}^T \\ &= \boldsymbol{\Gamma}_1 \boldsymbol{\Omega}_1 \boldsymbol{\Gamma}_1^T + \boldsymbol{\Gamma}_0 \boldsymbol{\Omega}_0 \boldsymbol{\Gamma}_0^T - \boldsymbol{\Gamma}_1 \boldsymbol{\Omega}_1 \boldsymbol{\eta} \boldsymbol{\Sigma}_Y^{-1} (\boldsymbol{\Gamma}_1 \boldsymbol{\Omega}_1 \boldsymbol{\eta})^T \\ &= \boldsymbol{\Gamma}_1 (\boldsymbol{\Omega}_1 - (\boldsymbol{\Omega}_1 \boldsymbol{\eta}) \boldsymbol{\Sigma}_Y^{-1} (\boldsymbol{\Omega}_1 \boldsymbol{\eta})^T) \boldsymbol{\Gamma}_1^T + \boldsymbol{\Gamma}_0 \boldsymbol{\Omega}_0 \boldsymbol{\Gamma}_0^T \\ &\equiv \boldsymbol{\Gamma}_1 \boldsymbol{\Omega}_1^* \boldsymbol{\Gamma}_1^T + \boldsymbol{\Gamma}_0 \boldsymbol{\Omega}_0 \boldsymbol{\Gamma}_0^T, \end{aligned}$$

showing that $\boldsymbol{\Sigma}_{X|Y}$ has the same decomposition as $\boldsymbol{\Sigma}_X$, but the material variation $\boldsymbol{\Omega}_1^* = \boldsymbol{\Omega}_1 - (\boldsymbol{\Omega}_1 \boldsymbol{\eta}) \boldsymbol{\Sigma}_Y^{-1} (\boldsymbol{\Omega}_1 \boldsymbol{\eta})^T$ has been reduced by the variation explained by \mathbf{Y} . Next, given the regression equation $\vec{X}(s)|\vec{Y}(s) = \vec{\mu}_{X|Y} +$

$\beta_X^T \vec{Y} + \vec{\epsilon}_{X|Y}(s)$ the reverse regression coefficients β_X can be written as

$$\begin{aligned}\beta_X &= \Sigma_Y^{-1} \Sigma_{XY}^T \\ &= \Sigma_Y^{-1} (\Gamma_1 \Omega_1 \eta)^T \\ &\equiv (\Gamma_1 \eta_X)^T,\end{aligned}$$

where $\eta_X = \Omega_1 \eta \Sigma_Y^{-1}$, showing that β_X has the same form as β .

Using properties of the Kronecker product, $|\Sigma_{X|Y} \otimes \rho(\theta)| = |\Sigma_{X|Y}|^n |\rho(\theta)|^p$.

Finally, because Γ_1, Γ_0 are orthogonal, $|\Sigma_{X|Y}| = |\Omega_1^*| |\Omega_0|$.

Now prepared to embark, the log-likelihood can be written as

$$\begin{aligned}L(\mathbf{X}, \mathbf{Y}) &= -\frac{n}{2} |\Sigma_{X|Y}| - \frac{1}{2} \text{vec}(\mathbf{X} - \vec{1} \vec{\mu}_{X|Y}^T - \mathbf{Y} \beta_X)^T (\Sigma_{X|Y} \otimes \rho(\theta))^{-1} \text{vec}(\mathbf{X} - \vec{1} \vec{\mu}_{X|Y}^T - \mathbf{Y} \beta_X) \\ &\quad - \frac{n(p+r)}{2} \log(2\pi) - \frac{p+r}{2} |\rho(\theta)| \\ &\quad - \frac{n}{2} |\Sigma_Y| - \frac{1}{2} \text{vec}(\mathbf{Y} - \vec{1} \vec{\mu}_Y^T)^T (\Sigma_Y \otimes \rho(\theta))^{-1} \text{vec}(\mathbf{Y} - \vec{1} \vec{\mu}_Y^T) \\ &= -\frac{n}{2} |\Omega_1^*| - \frac{1}{2} \text{vec}(\mathbf{X} \Gamma_1 - \vec{1} \vec{\mu}_{X|Y}^T \Gamma_1 - \mathbf{Y} \eta_X^T) (\Omega_1^* \otimes \rho(\theta))^{-1} \text{vec}(\mathbf{X} \Gamma_1 - \vec{1} \vec{\mu}_{X|Y}^T \Gamma_1 - \mathbf{Y} \eta_X^T) \\ &\quad - \frac{n}{2} |\Omega_0| - \frac{1}{2} \text{vec}(\mathbf{X} \Gamma_0 - \vec{1} \vec{\mu}_{X|Y}^T \Gamma_0) (\Omega_0 \otimes \rho(\theta))^{-1} \text{vec}(\mathbf{X} \Gamma_0 - \vec{1} \vec{\mu}_{X|Y}^T \Gamma_0) \\ &\quad - \frac{n(p+r)}{2} \log(2\pi) - \frac{p+r}{2} |\rho(\theta)| \\ &\quad - \frac{n}{2} |\Sigma_Y| - \frac{1}{2} \text{vec}(\mathbf{Y} - \vec{1} \vec{\mu}_Y^T)^T (\Sigma_Y \otimes \rho(\theta))^{-1} \text{vec}(\mathbf{Y} - \vec{1} \vec{\mu}_Y^T).\end{aligned}$$

Let $\vec{\mu}_1 = \Gamma_1 \vec{\mu}_{X|Y}$ and $\vec{\mu}_0 = \Gamma_0 \vec{\mu}_{X|Y}$. Taking derivatives and equating to zero

shows maximums are achieved at

$$\begin{aligned}
\hat{\mathbf{B}}_1 &\equiv \begin{bmatrix} \hat{\mu}_1 \\ \hat{\boldsymbol{\eta}}_X \end{bmatrix} = \left((\tilde{\mathbf{Y}}^T \boldsymbol{\rho}(\theta)^{-1} \tilde{\mathbf{Y}})^{-1} \tilde{\mathbf{Y}}^T \boldsymbol{\rho}(\theta)^{-1} \mathbf{X} \boldsymbol{\Gamma}_1 \right)^T \\
\hat{\mu}_0 &= \left((\vec{\mathbf{1}}^T \boldsymbol{\rho}(\theta)^{-1} \vec{\mathbf{1}})^{-1} \vec{\mathbf{1}}^T \boldsymbol{\rho}(\theta)^{-1} \mathbf{X} \boldsymbol{\Gamma}_1 \right)^T \\
\hat{\mu}_Y &= \left((\vec{\mathbf{1}}^T \boldsymbol{\rho}(\theta)^{-1} \vec{\mathbf{1}})^{-1} \vec{\mathbf{1}}^T \boldsymbol{\rho}(\theta)^{-1} \mathbf{Y} \right)^T \\
\hat{\boldsymbol{\Omega}}_1^* &= (\mathbf{X} \boldsymbol{\Gamma}_1 - \tilde{\mathbf{Y}} \hat{\mathbf{B}}_1^T)^T \boldsymbol{\rho}(\theta)^{-1} (\mathbf{X} \boldsymbol{\Gamma}_1 - \tilde{\mathbf{Y}} \hat{\mathbf{B}}_1^T) \\
&= \boldsymbol{\Gamma}_1^T \mathbf{S}_{X|Y}(\theta) \boldsymbol{\Gamma}_1 \\
\hat{\boldsymbol{\Omega}}_0 &= (\mathbf{X} \boldsymbol{\Gamma}_0 - \vec{\mathbf{1}} \hat{\mu}_0^T)^T \boldsymbol{\rho}(\theta)^{-1} (\mathbf{X} \boldsymbol{\Gamma}_0 - \vec{\mathbf{1}} \hat{\mu}_0^T) \\
&= \boldsymbol{\Gamma}_0^T \mathbf{S}_X(\theta) \boldsymbol{\Gamma}_0 \\
\hat{\boldsymbol{\Sigma}}_Y &= (\mathbf{Y} - \vec{\mathbf{1}} \hat{\mu}_Y^T)^T \boldsymbol{\rho}(\theta)^{-1} (\mathbf{Y} - \vec{\mathbf{1}} \hat{\mu}_Y^T) \\
&= \mathbf{S}_Y(\theta),
\end{aligned}$$

where $\mathbf{S}_{X|Y}(\theta)$, $\mathbf{S}_X(\theta)$ and $\mathbf{S}_Y(\theta)$ are the sample covariance matrices defined in Equations 16. Substituting these quantities into the log-likelihood gives the partially maximized log-likelihood

$$\begin{aligned}
L_1(\mathbf{X}, \mathbf{Y}) &= -\frac{n}{2} \log |\boldsymbol{\Gamma}_1^T \mathbf{S}_{X|Y}(\theta) \boldsymbol{\Gamma}_1| - \frac{n}{2} \log |\boldsymbol{\Gamma}_0^T \mathbf{S}_X(\theta) \boldsymbol{\Gamma}_0| - \frac{n}{2} \log |\mathbf{S}_Y(\theta)| - \frac{p+r}{2} \log |\boldsymbol{\rho}(\theta)| \\
&\quad - \frac{n(p+r)}{2} \log(2\pi + 1).
\end{aligned}$$

To arrive at objective function 15, make the substitution

$$\log |\mathbf{\Gamma}_0^T \mathbf{S}_X(\theta) \mathbf{\Gamma}_0| = \log |\mathbf{\Gamma}_1^T \mathbf{S}_X(\theta)^{-1} \mathbf{\Gamma}_1| + \log |\mathbf{S}_X(\theta)|,$$

(see (Cook, 2018, Lemma A.13)):

$$\begin{aligned} L_1(\mathbf{X}, \mathbf{Y}) = & -\frac{n}{2} \log |\mathbf{\Gamma}_1^T \mathbf{S}_{X|Y}(\theta) \mathbf{\Gamma}_1| - \frac{n}{2} \log |\mathbf{\Gamma}_1^T \mathbf{S}_X(\theta)^{-1} \mathbf{\Gamma}_1| \\ & - \frac{n}{2} \log |\mathbf{S}_X(\theta)| - \frac{n}{2} \log |\mathbf{S}_Y(\theta)| - \frac{p+r}{2} \log |\boldsymbol{\rho}(\theta)| - \frac{n(p+r)}{2} \log(2\pi + 1). \end{aligned}$$

Still left to be estimated are the regression coordinates $\boldsymbol{\eta}$. Here, reverse the conditioning $L(\mathbf{X}, \mathbf{Y}) = L(\mathbf{Y}|\mathbf{X}) + L(\mathbf{X})$. Parameter $\boldsymbol{\eta}$ appears only in $L(\mathbf{Y}|\mathbf{X})$, so the second term can be dropped. Differentiating with respect to $\boldsymbol{\eta}$ and equating to zero gives $\hat{\boldsymbol{\eta}} = \hat{\mathbf{\Gamma}}_1^T \hat{\boldsymbol{\beta}}_{\text{GLS}^*}$, where GLS coefficients $\hat{\boldsymbol{\beta}}_{\text{GLS}^*}$ are given in Equations 17.

8.2 Potential Gains

The results 21 and 20 are proven here. For convenience of notation, we temporarily assume the intercept term is zero in the regression $\vec{Y}(s)|\vec{X}(s)$ and the spatial parameter θ is dropped from $\boldsymbol{\rho}(\theta)$. Recall it is assumed that $\mathbf{\Gamma}_1$ and θ are known.

To prove 21, the law of total variance is first applied

$$\text{Var}[\text{vec}(\hat{\boldsymbol{\beta}}_{\text{GLS}})] = \text{Var}[\text{E}[\text{vec}(\hat{\boldsymbol{\beta}}_{\text{GLS}})|\mathbf{X}]] + \text{E}[\text{Var}[\text{vec}(\hat{\boldsymbol{\beta}}_{\text{GLS}})|\mathbf{X}]].$$

Since $E[\text{vec}(\hat{\boldsymbol{\beta}}_{\text{GLS}})|\mathbf{X}] = \boldsymbol{\beta}$, the first term is zero. Continuing,

$$\begin{aligned}
\text{Var}[\text{vec}(\hat{\boldsymbol{\beta}}_{\text{GLS}})] &= E[\text{Var}[\text{vec}(\hat{\boldsymbol{\beta}}_{\text{GLS}})|\mathbf{X}]] \\
&= E[\text{Var}[\text{vec}((\mathbf{X}^T \boldsymbol{\rho}^{-1} \mathbf{X})^{-1} \mathbf{X}^T \boldsymbol{\rho}^{-1} \mathbf{Y})|\mathbf{X}]] \\
&= E[\text{Var}[(\mathbf{I}_r \otimes (\mathbf{X}^T \boldsymbol{\rho}^{-1} \mathbf{X})^{-1} \mathbf{X}^T \boldsymbol{\rho}^{-1}) \text{vec}(\mathbf{Y})|\mathbf{X}]] \\
&= E[(\mathbf{I}_r \otimes (\mathbf{X}^T \boldsymbol{\rho}^{-1} \mathbf{X})^{-1} \mathbf{X}^T \boldsymbol{\rho}^{-1}) (\boldsymbol{\Sigma}_{Y|X} \otimes \boldsymbol{\rho}) (\mathbf{I}_r \otimes (\mathbf{X}^T \boldsymbol{\rho}^{-1} \mathbf{X})^{-1} \mathbf{X}^T \boldsymbol{\rho}^{-1})^T] \\
&= E[\boldsymbol{\Sigma}_{Y|X} \otimes (\mathbf{X}^T \boldsymbol{\rho}^{-1} \mathbf{X})^{-1}].
\end{aligned}$$

Since $\text{Var}[\text{vec}(\mathbf{X})] = \boldsymbol{\Sigma}_X \otimes \boldsymbol{\rho}$, matrix $\mathbf{X}^* = \boldsymbol{\rho}^{-1/2} \mathbf{X}$ is equivalent to a matrix of n independent observations of a multivariate normal distribution with variance $\boldsymbol{\Sigma}_X$. Therefore $(\mathbf{X}^T \boldsymbol{\rho}^{-1} \mathbf{X})^{-1} = (\mathbf{X}^{*T} \mathbf{X}^*)^{-1}$ follows an Inverse-Wishart distribution with expected value $\frac{1}{n-p-2} \boldsymbol{\Sigma}_X^{-1}$, proving 21.

To prove 20, first note that $\boldsymbol{\eta}$ is the regression coefficients for $\vec{Y}(s)|\boldsymbol{\Gamma}_1^T \vec{X}(s)$ and $\hat{\boldsymbol{\eta}} = (\boldsymbol{\Gamma}_1^T \mathbf{X}^T \boldsymbol{\rho}^{-1} \mathbf{X} \boldsymbol{\Gamma}_1)^{-1} \boldsymbol{\Gamma}_1^T \mathbf{X}^T \boldsymbol{\rho}^{-1} \mathbf{Y}$. Matrix $\boldsymbol{\rho}^{-1/2} \mathbf{X} \boldsymbol{\Gamma}_1$ is equivalent to a matrix of n independent observations of a multivariate normal distribution with variance $\boldsymbol{\Omega}_1$. Therefore, by the same logic as above

$$\text{Var}[\text{vec}(\hat{\boldsymbol{\eta}})] = \left(\frac{1}{n-u-2} \right) \boldsymbol{\Sigma}_{Y|X} \otimes \boldsymbol{\Omega}_1,$$

and therefore

$$\begin{aligned}
\text{Var}[\text{vec}(\hat{\boldsymbol{\beta}})] &= \text{Var}[\text{vec}(\boldsymbol{\Gamma}_1 \hat{\boldsymbol{\eta}})] \\
&= \left(\frac{1}{n-u-2} \right) \boldsymbol{\Sigma}_{Y|X} \otimes \boldsymbol{\Gamma}_1 \boldsymbol{\Omega}_1 \boldsymbol{\Gamma}_1^T,
\end{aligned}$$

proving 20.

8.3 Asymptotic Distributions

Proof of Theorem 2

Let \mathbf{E}_p be the $p^2 \times p(p+1)/2$ expansion matrix (sometimes called the duplication matrix) such that for any symmetric $p \times p$ matrix \mathbf{M} , we have $\mathbf{E}_p \text{vech}(\mathbf{M}) = \text{vec}(\mathbf{M})$. Similarly, let \mathbf{C}_p be the $p(p+1)/2 \times p^2$ contraction matrix (elimination matrix) such that $\mathbf{C}_p \text{vec}(\mathbf{M}) = \text{vech}(\mathbf{M})$.

Assume spatial parameters θ are known. Let L be the log-likelihood of the full spatial model with no dimension reduction defined by Equations 10 and \mathbf{Z} be the $n \times k$ observation matrix for $\vec{Z}(s)$, where k is the dimension of $\vec{Y}(s)$ plus the dimension of $\vec{X}(s)$:

$$L(\boldsymbol{\Sigma}_Z, \mu_Z | \mathbf{Z}) = -\frac{n}{2} \log |\boldsymbol{\Sigma}_Z| - \frac{k}{2} \log |\boldsymbol{\rho}_\theta| - \frac{1}{2} \text{vec}(\mathbf{Z} - \vec{1}_n \vec{\mu}_Z^T)^T (\boldsymbol{\Sigma}_Z \otimes \boldsymbol{\rho}_\theta)^{-1} \text{vec}(\mathbf{Z} - \vec{1}_n \vec{\mu}_Z^T).$$

With some linear algebra, this can be rewritten as

$$L(\boldsymbol{\Sigma}_Z, \mu_Z | \mathbf{Z}) = -\frac{n}{2} \log |\boldsymbol{\Sigma}_Z| - \frac{k}{2} \log |\boldsymbol{\rho}_\theta| - \frac{1}{2} \text{trace}[\mathbf{R}^T \boldsymbol{\rho}_\theta^{-1} \mathbf{R} \boldsymbol{\Sigma}_Z^{-1}].$$

where $\mathbf{R} = \mathbf{Z} - \vec{1}_n \vec{\mu}_Z^T$ is the centered observation matrix. Let $\mathbf{R}_\theta = \boldsymbol{\rho}_\theta^{-1/2} \mathbf{R}$ and $\mathbf{S}_\theta = \frac{1}{n} \mathbf{R}_\theta^T \mathbf{R}_\theta = \frac{1}{n} \mathbf{R}^T \boldsymbol{\rho}_\theta^{-1} \mathbf{R}$. Rewriting the log-likelihood with this re-

placement gives

$$L(\boldsymbol{\Sigma}_Z, \mu_Z | \mathbf{Z}) = -\frac{n}{2} \log |\boldsymbol{\Sigma}_Z| - \frac{k}{2} \log |\boldsymbol{\rho}_\theta| - \frac{n}{2} \text{trace}[\mathbf{S}_\theta \boldsymbol{\Sigma}_Z^{-1}].$$

Note that

$$\mathbf{E}[\mathbf{R}_\theta] = \boldsymbol{\rho}_\theta^{-1/2} \mathbf{E}[\mathbf{R}] = \mathbf{0},$$

and that

$$\begin{aligned} \text{Var}[\text{vec}(\mathbf{R}_\theta)] &= \text{Var}[(\mathbf{I}_k \otimes \boldsymbol{\rho}_\theta^{-1/2}) \text{vec}(\mathbf{R})] \\ &= (\mathbf{I}_k \otimes \boldsymbol{\rho}_\theta^{-1/2}) (\boldsymbol{\Sigma}_Z \otimes \boldsymbol{\rho}_\theta) (\mathbf{I}_k \otimes \boldsymbol{\rho}_\theta^{-1/2})^T \\ &= (\boldsymbol{\Sigma}_Z \otimes \mathbf{I}_n). \end{aligned}$$

Therefore the n rows of \mathbf{R}_θ are equivalent to n independent observations of the multivariate normal distribution $N(\mathbf{0}, \boldsymbol{\Sigma}_Z)$ and $\mathbf{E}[\mathbf{S}_\theta] = \boldsymbol{\Sigma}_Z$. The term $-\frac{k}{2} \log |\boldsymbol{\rho}_\theta|$ in the log-likelihood disappears upon differentiation with respect to $\text{vech}(\boldsymbol{\Sigma}_Z)$, leading to the same information matrix for $\text{vech}(\boldsymbol{\Sigma}_Z)$ as the multivariate normal distribution with independent observations, specifically

$$\mathbf{J}_\Sigma = \frac{1}{2} \mathbf{E}_k^T (\boldsymbol{\Sigma}_Z^{-1} \otimes \boldsymbol{\Sigma}_Z^{-1}) \mathbf{E}_k.$$

The parameters of $h(\psi)$ are functions of $\boldsymbol{\Sigma}_Z$ and have the same information matrix \mathbf{J}_F as in Cook et al. (2013). Additionally, the mapping $\psi \rightarrow h(\psi)$ is the same as in Cook et al. (2013). Therefore the derivation of the asymptotic

distributions follows Cook et al. (2013) exactly, yielding Theorem 2.

Proof of Theorem 3

$$\mathbf{J}_F^{-1} - \mathbf{J}_{\text{SPE}}^{-1} = \mathbf{J}_F^{-1/2} \left(\mathbf{I} - \mathbf{J}_F^{1/2} \mathbf{H} (\mathbf{H}^T \mathbf{J}_F \mathbf{H})^\dagger \mathbf{H}^T \mathbf{J}_F^{1/2} \right) \mathbf{J}_F^{-1/2} \quad (26)$$

$$= \mathbf{J}_F^{-1/2} \mathbf{P}_* \mathbf{J}_F^{-1/2} \geq 0. \quad (27)$$

Matrix \mathbf{P}_* is the orthogonal projection onto the orthogonal complement of the column space of $\mathbf{J}^{1/2} \mathbf{H}$. Since $\mathbf{P}_* = \mathbf{P}_* \mathbf{P}_*$, we have $|\mathbf{P}_*| = |\mathbf{P}_*|^2$ implying $|\mathbf{P}_*| \geq 0$. Matrix \mathbf{P}_* is therefore semi-positive definite, making $\mathbf{J}_F^{-1/2} \mathbf{P}_* \mathbf{J}_F^{-1/2}$ semi-positive definite. This proves the envelope estimator is asymptotically efficient versus the full GLS estimator.

8.4 Simulation Results

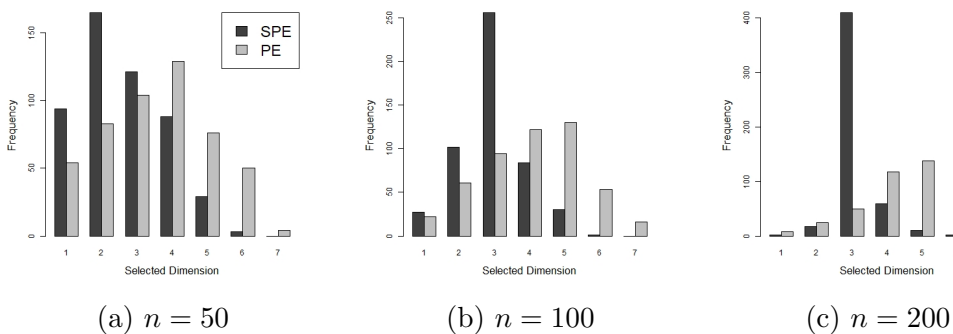
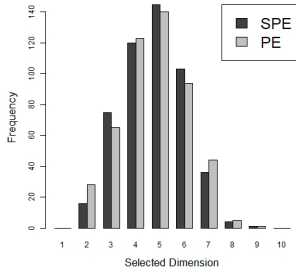
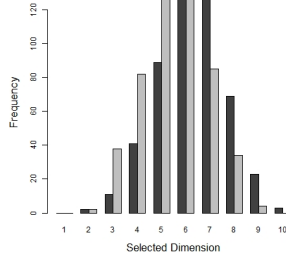


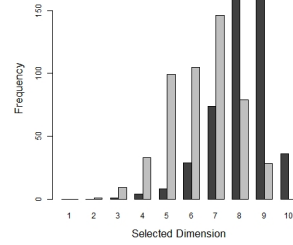
Figure 4: Histograms of estimated envelope dimensions for Simulation 2: $u < p$ and $\|\Omega_0\| \ll \|\Omega_1\|$.



(a) $n = 50$

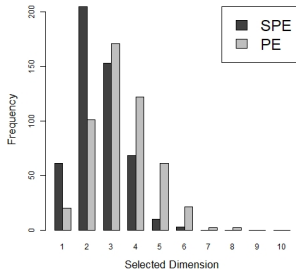


(b) $n = 100$

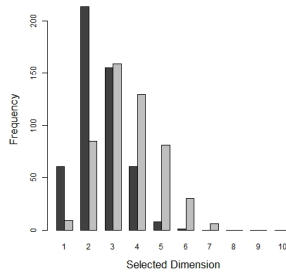


(c) $n = 200$

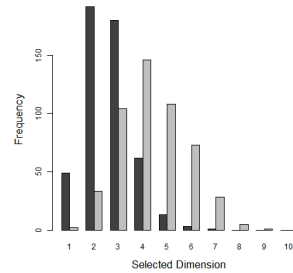
Figure 5: Histograms of estimated envelope dimensions for Simulation 3: $u = p$.



(a) $n = 50$



(b) $n = 100$



(c) $n = 200$

Figure 6: Histograms of estimated envelope dimensions for Simulation 4: $u < p$ and $\|\Omega_1\| \approx \|\Omega_0\|$.

8.5 Data Analysis

Traditional multivariate techniques cannot be directly applied to compositional data because of the variable constraints: all variables for a given observation sum to unity. Thus, it has become common to analyze the log-ratios of the components. Let $\vec{Z} = [Z_1, \dots, Z_k]$ be a k -dimensional composition (or subcomposition). Then the $k - 1$ dimensional transformed variable

$$\vec{X} = [\log(Z_1/Z_k) \ \log(Z_2/Z_k) \ \cdots \ \log(Z_{k-1}/Z_k)]^T,$$

is unconstrained. Furthermore, if the composition \vec{Z} is assumed to follow a logistic normal distribution, then \vec{X} follows a multivariate normal distribution. The choice of denominator in the ratio, given above as the last component of the composition, is arbitrary, and equivalent inference is obtained for any choice of denominator (Aitchison, 1982, Chapter 5).

For the data analysis in this paper, the predictors were chosen to be the relative log-concentrations of the major chemical elements. Let $\text{MCE}_1, \dots, \text{MCE}_{11}$ represent the eleven major chemical elements. The major chemical elements are examined as a subcomposition, with

$$Z_j = \text{MCE}_j / \left(\sum_{w=1}^{11} \text{MCE}_w \right),$$

normalizing so that the relative proportions of the major chemical elements are studied. The major chemical elements are normalized as a separate sub-

composition in order to remove any trivial, compositional relationships between the predictors and the response, for example, an increase in potassium oxide concentration causes a decrease in REE concentration simply by leaving less room in the composition. Rather, the goal is to analyze the effect of the relative proportions of major chemical elements on the REE concentration, for example, an increase in potassium oxide relative to the other major chemical elements makes higher REE concentrations likely. To remove the constraints on the predictors, a log-ratio transformation is applied

$$X_j = \log(Z_j/Z_{11}), \quad j = 1, \dots, 10$$

leaving $p = 10$ predictor variables, with major chemical element aluminum oxide (Al_2O_3) arbitrarily chosen as the denominator.

The REE element concentrations are represented in parts per million, between 0 and 10^6 . The regression response is chosen to be the log-concentration of REEs relative to all other parts of the composition

$$Y = \log(REE/(10^6 - REE)).$$

a monotone increasing transformation that gives a response that is unconstrained, interpretable and congruent with the goals of the analysis.

Some of the observations had chemical element concentrations below the detection threshold of the instrument used to analyze the sample. Specifically, three samples had a major chemical element titanium dioxide (TiO_2)

below the detection threshold and ten samples had at least one rare earth element below the detection threshold. Rather than omit these samples, the values were replaced with half of the detection threshold. Because so few samples had a major chemical element below the detection threshold, and any REE below the detection threshold will have little impact on the total REE concentration, this choice of replacement had little impact when compared to any other reasonable replacement scheme.